HHS Public Access

Author manuscript

Genet Med. Author manuscript; available in PMC 2023 December 01.

Published in final edited form as:

Genet Med. 2022 December ; 24(12): 2501–2515. doi:10.1016/j.gim.2022.08.025.

The p190 RhoGAPs, *ARHGAP35* and *ARHGAP5*, are Implicated in GnRH Neuronal Development: Evidence from Patients with Idiopathic Hypogonadotropic Hypogonadism, Zebrafish and *in vitro* GAP Activity Assay

Margaret F. Lippincott[1], **Wanxue Xu**[1], **Abigail A. Smith**[2,3], **Xinyu Miao**[4], **Agathe Lafont**[5], **Omar Shennib**[3], **Gordon J. Farley**[1], **Riwa Sabbagh**[1], **Angela Delaney**[6], **Maria Stamou**[1], **Lacey Plummer**[1], **Kathryn Salnikov**[1], **Neoklis A. Georgopoulos**[7], **Veronica Mericq**[8], **Richard Quinton**[9], **Frederic Tran Mau-Them**[10], **Sophie Nambot**[11], **Asma Hamad**[12], **Helen Brittain**[12], **Rebecca S. Tooze**[13], **Eduardo Calpena**[13], **Andrew O.M. Wilkie**[13], **Marjolaine Willems**[14], **William F. Crowley**[15], **Ravikumar Balasubramanian**[1], **Nathalie Lamarche-Vane**[4], **Erica E. Davis**[2,3], **Stephanie B. Seminara**[1]

[1]Reproductive Endocrine Unit, Massachusetts General Hospital, Boston, MA 02114, USA

[2]Department of Pediatrics and Department of Cell and Developmental Biology, Feinberg School of Medicine, Northwestern University, Chicago, IL, 60611

[3]Stanley Manne Children's Research Institute, Ann & Robert H. Lurie Children's Hospital of Chicago, Chicago, IL, 60611

[4]Cancer Research Program, Research Institute of the McGill University Health Centre, Department of Anatomy and Cell Biology, McGill University, Montréal, QC H4A 3J1, Canada

[5]Center for Human Disease Modeling, Duke University Medical Center, Durham, NC 27701, USA

[6]National Institutes of Health, Intramural Research Program, Bethesda, MD 20892, USA

[7]Division of Endocrinology-Department of Internal Medicine, University of Patras School of Health Sciences, Rio-Patras, Greece

Correspondence regarding this manuscript should be sent to Margaret Lippincott, mlippincott@mgh.harvard.edu; Massachusetts General Hospital, 55 Fruit Street, Bartlett Hall Extension 5th Floor, Boston, MA, 02114; 617-726-8434.

Author Contributions: Conceptualization (M.F.L.,W.F.C., N.L-V., E.E.D.), Data Curation (M.F.L., W.X., A.A.S., X.M., N.A.G., M.S., L.P., K.S., V.M., R.Q., W.F.C., R.B., N.L-V., E.E.D., S.B.S.), Formal analysis (M.F.L., W.X., A.A.S., X.M., O.S., G.J.F., R.S., A.D., M.S., F.T.M-T., S.N., A.H., H.B., R.S.T., E.C., A.O.M.W., M.W., N.L-V., E.E.D.), Funding acquisition (M.F.L., A.O.M.W., W.F.C., R.B., N.L-V., S.B.S.), Investigation (M.F.L., W.X., A.A.S., X.M., A.L., O.S., G.J.F., R.S., A.D., N.A.G., M.S., L.P., V.M., R.Q., F.TM-T., S.N., A.H., H.B., R.S.T., E.C., A.O.M.W., R.B., N.L-V., E.E.D), Methodology (M.F.L., W.X., A.L., N.L-V., E.E.D.), Project administration (M.F.L., W.F.C., N.L-V., E.E.D., S.B.S.), Resources (M.F.L., N.A.G., M.S., V.M., R.Q., F.T.M-T., S.N., A.H., H.B., M.W., W.F.C., R.B., N.L-V., E.E.D., S.B.S), Supervision (M.F.L., W.F.C., R.B., L.M-V., E.E.D., S.B.S.), Validation (M.F.L., W.X., N.L-V., E.E.D.), Visualization (M.F.L., W.X., A.A.S., X.M., A.D., E.E.D.), Writing-original draft (M.F.L., W.X., X.M., M.W., W.F.C., N.L-V., E.E.D.), Writing-review and editing (M.F.L., W.X., A.A.S., A.L., O.S., G.J.F., R.S., A.D., N.A.G., M.S., L.P., K.S., V.M., R.Q., F.T.M-T., S.N., A.H., H.B., R.S.T., E.C., A.O.M.W., W.F.C., R.B., N.L-V., E.E.D., S.B.S.).

Ethics Declaration: The Massachusetts General Hospital Partners Institutional Review Board approved all human subjects research. Subjects participated in this study following their informed consent. Based on the consent form used for human subject research, individual-level data, including clinical data, was de-identified for this report. Subjects matched through GeneMatcher provided consent to their local institution to share de-identified data for publication. All studies employing zebrafish were approved by the Duke University or Northwestern University Institutional Animal Care and Use Committees.

Disclosures: The authors declare no conflict of interest

[8.]Instituto de Investigaciones Materno Infantil (IDIMI), University of Chile, Santiago, Chile

[9.]Translational & Clinical Research Institute, University of Newcastle-upon-Tyne, Newcastle-upon-Tyne, UK

[10.]Functional Unit 6254 Innovation in Genomic Diagnosis of Rare Diseases, CHU Dijon Bourgogne, Dijon, France.

[11.]Centre de Référence Maladies Rares « Anomalies du Développement Et Syndrome Malformatifs » de L'Est, Hôpital D'Enfants, FHU-TRANSLAD, CHU Dijon Bourgogne, 21000, Dijon, France.

[12.]West Midlands Regional Genetics Service, Birmingham Women and Children's Hospital NHS Foundation Trust, Birmingham, UK

[13.]Clinical Genetics Group, MRC Weatherall Institute of Molecular Medicine, University of Oxford, Oxford, UK

[14.]Medical Genetic Department for Rare Diseases and Personalized Medicine, Reference Center AD SOOR, AnDDI-RARE, Groupe DI, Inserm U1298, INM, Montpellier University, Centre Hospitalier Universitaire de Montpellier, Montpellier, France

[15.]The Endocrine Unit, Massachusetts General Hospital, Boston, MA 02114, USA

Abstract

Purpose: To identify novel genes for Isolated Hypogonadotropic Hypogonadism (IHH).

Methods: A cohort of 1,387 probands with IHH underwent exome sequencing and *de novo*, familial and cohort-wide investigations. Functional studies were performed on two p190 Rho-GTPase Activating Proteins (p190 RhoGAP), *ARHGAP35* and *ARHGAP5*, which involved *in vivo* modeling in larval zebrafish and an *in vitro* p190A-GAP activity assay.

Results: Rare protein-truncating variants (PTV; n=5) and missense variants in the RhoGAP domain (n=7) in *ARHGAP35* were identified in IHH cases [rare variant enrichment: PTV (unadjusted p=3.1E-06) and missense (adjusted p=4.9E-03) vs. controls]. Zebrafish modeling using gnrh3:egfp phenotype assessment demonstrated that mutant larvae with deficient *arhgap35a*, the predominant ARHGAP35 paralog in the zebrafish brain, display decreased GnRH3-GFP+ neuronal area, a read-out for IHH. *In vitro* GAP activity studies demonstrated that one rare missense variant (*ARHGAP35* p.(Arg1284Trp)) had decreased GAP activity. Rare PTVs (n=2) also were discovered in *ARHGAP5*, a paralog of *ARHGAP35*; however, *arhgap5* zebrafish mutants did not display significant GnRH3-GFP+ abnormalities.

Conclusion: This study identified *ARHGAP35* as a new autosomal dominant genetic driver for IHH and *ARHGAP5* as a candidate gene for IHH. These observations suggest a novel role for the p190 RhoGAP proteins in GnRH neuronal development and integrity.

Keywords

GnRH; puberty; idiopathic hypogonadotropic hypogonadism; IHH; developmental disorder; intellectual disability; ARHGAP35; ARHGAP5; p190; p190A; p190B; Rho-GTPases; RhoGAPs; Rho-GTPase activating protein

INTRODUCTION

Individuals with isolated hypogonadotropic hypogonadism (IHH) present with a failure to enter or progress through puberty resulting in sexual infantilism and infertility in the absence of medication[1]. IHH is a rare, heterogeneous, predominantly Mendelian disorder whose pathomechanism is defects in the biosynthesis, secretion, or action of gonadotropin-releasing hormone (GnRH).[1,2] These genetic defects can result in impairment of embryonic development and can prevent GnRH neuronal differentiation from stem cells within the developing olfactory epithelium, or the subsequent migration of GnRH neurons into the hypothalamus of the central nervous system (CNS). GnRH neuronal ontology is part of a shared embryonic developmental program intersecting olfactory, craniofacial and CNS development. As a result, IHH has served as a valuable human disease model to discover genes that yield insights into not only GnRH neuron development, migration, and action but also their role in developmental pleiotropy across organ systems.[3–6]

The current report identifies an excess burden of rare variants in two p190-Rho GTPase-activating proteins (RhoGAPs), *ARHGAP35,* and *ARHGAP5* through familial, *de novo* and cohort-wide investigations in a large ensemble of individuals with IHH. The p190 RhoGAPs, *ARHGAP35* and *ARHGAP5*, are evolutionarily conserved, intolerant to genetic variation, and critically important for brain development.[7–11] p190 RhoGAPs are key negative regulators of RhoGTPase (e.g., RhoA) functions: neuronal differentiation, axonal guidance, and adhesion-mediated signaling.[7–9] As such, p190RhoGAPs, regulate pathways where protein-truncating variants (PTVs) result in haploinsufficiency and IHH.[12,13]

To understand the human genetic evidence, GnRH development was assessed in stable *ARHGAP35* and *ARHGAP5* zebrafish mutants. A p190A-GAP assay was employed to measure GAP activity in *ARHGAP35* missense variants. Further, using GeneMatcher, we aggregated additional individuals bearing heterozygous PTVs in *ARHGAP35,* providing human genetic and phenotypic evidence that ARHGAP35 plays a pleiotropic role during development resulting in autosomal dominant IHH and neurodevelopmental disorders (DD).[14,15]

METHODS

Patient cohorts

Patients with IHH were enrolled in a genetic study at Massachusetts General Hospital as previously described (n =1387 probands, n=350 parents; Supplementary Methods).[16] GeneMatcher facilitated the identification of patients in other cohorts with PTVs in *ARHGAP35.*[15]

Exome Sequencing (ES) was performed using The Broad Institute Genomics Platform in 1,387 patients with IHH and 350 parents, generating 175 trios. Variant calling was performed as previously described[4]. Rare sequence variants (RSVs) were required to: be non-synonymous variants (stop gain, frameshift, or missense) or canonical splice altering variants (± 2 base-pairs from exon-intron boundaries); have a minor allele frequency (MAF) of <0.1% in the genome Aggregation Database (gnomAD) based on maximum MAF across

all population sub-groups; a quality depth >5; a call rate >0.95; MEDIUM or HIGH impact as annotated by Ensembl Variant Effect Predictor; and predicted as damaging in ≥ 2 prediction programs.[17–19] Copy number variant (CNV) calls were conducted from ES using the GATK-gCNV pipeline as previously described.[20] CNVs present in known IHH genes (MAF <1%) were curated[20] (Supplementary Methods and Supplementary Table 1).

Identification of Variants of Interest:

We conducted two family-based analyses. In the first, we started with three affected family members in two generations and examined ES data for segregating: a) RSVs in known IHH genes; b) heterozygous RSVs and c) homozygous RSVs, including the rare possibility of uniparental isodisomy. Segregation was defined as being present in the affected individual(s) in the family. RSVs were considered "RSVs of interest" if they were PTVs, absent from public databases (i.e. gnomAD), and under genic constraint as defined by gnomAD. In the second family, we analyzed a trio for "RSVs of interest" that were *de novo*. We then evaluated these discoveries in an IHH cohort (n=1,387) using gene-based burden testing to determine if the gene was enriched for variation in our IHH cohort compared with gnomAD.[10,16] All RSVs were confirmed using bi-directional Sanger sequencing in all probands and available family members.

Pathway analysis was completed using STRING v.11.5.[21] All active, high confidence interaction scores in the whole STRING network were analyzed, and up to 50 first shell interactors were graphed for networks seeded with *ARHGAP35* alone, *ARHGAP5* alone, or known IHH genes, *ARHGAP35*, and *ARHGAP5*.

Zebrafish husbandry:

Transgenic *gnrh3:gfp*[22] adult fish were maintained in standard conditions with a 14h light-10h dark cycle, and embryos were collected from natural matings of adult fish. Embryos and larvae were reared at 28.5°C in embryo medium (0.3 g/L NaLc, 75 mg/L $CaSO_4$, 37.5 mg/L $NaHCO_3$, and 0.003% methylene blue) until experimental endpoint.

CRISPR/Cas9 genome editing and stable zebrafish mutant lines:

To identify zebrafish orthologs for genome editing, we performed reciprocal BLAST searches between *Homo sapiens ARHGAP35* (GenBank IDs: NM_004491.5; NP_004482.4) or *ARHGAP5* (GenBank IDs: NM_001030055.2; NP_001025226.1) and the translated *Danio rerio* genome (GRCz11). Two zebrafish paralogs corresponding to ARHGAP35: *arhgap35a* (ENSDART00000154171.3) and *arhgap35b* (ENSDART00000084819.5); and ARHGAP5 (ENSDART00000086696.6) were targeted by single guide (sg) RNA sequences identified by ChopChop for CRISPR/Cas9 genome editing.[23] We synthesized sgRNAs using GeneArt Precision gRNA Synthesis Kit (ThermoFisher) according to the manufacturer's instructions. Mutant zebrafish lines for *arhgap35a, arhgap35b,* or *arhgap5* were established as previously described[3] (Supplementary Methods; Supplementary Table 2).

Quantitative reverse transcription (qRT)-PCR of endogenous zebrafish gene expression:

We evaluated the endogenous *arhgap35a, arhgap35b,* or *arhgap5* transcript amount in stable homozygous mutants for comparison with wild type (WT) siblings. At 2 days

post-fertilization (dpf), we decapitated larvae in biological triplicates with micro-scissors; individual tails were subjected to DNA extraction for genotyping, and same-genotype heads (30/pool) were combined for extraction of total RNA using Trizol (ThermoFisher) according to manufacturer's instructions. We reverse-transcribed cDNA using the QuantiTect Reverse Transcription Kit (Qiagen) per kit manual instructions using 1 μg total RNA. The resulting cDNA served as a template for each qRT-PCR reaction (30 ng cDNA template/reaction). All samples were analyzed in technical triplicates on a QuantStudio 3 real-time PCR system (ThermoFisher) using the Power SYBR Green PCR Master Mix (ThermoFisher) with three biological triplicates. The housekeeping gene *gapdh* was used to normalize gene-level expression using the $2^{-\Delta\Delta C}_{T}$ method.

Automated *in vivo* image acquisition and analysis of zebrafish larvae:

To quantify GnRH3 neuronal patterning in zebrafish larvae at 5 dpf, we performed automated imaging essentially as described.[4] (Supplementary Methods)

In vitro p190A GAP assay:

pGEX-6P1 plasmid encoding GST-tagged GAP domain of p190A was previously described.[24] Point variants were introduced into the WT form of p190A using the QuikChange II Site-Directed Mutagenesis Kit (Agilent) according to the manufacturer's instructions using custom-designed primers (Supplementary Table 3). All plasmids were verified by Sanger sequencing. Recombinant GST-tagged p190A-GAP WT and mutant proteins were expressed in BL21 (DE3) bacteria and purified using glutathione-agarose beads (Thermo Scientific) as described.[24] PreScission protease (GenScript) was used to cleave the GST tag. Eluted purified p190A-GAP proteins were concentrated using Amicon Ultra-4 centrifugal filters (Millipore), resolved by SDS-PAGE, and stained with Coomassie blue. Proteins were quantified using bovine serum albumin (BSA) as a standard. The GAP activity of p190A-GAP WT and mutant proteins was assessed using the RhoGAP assay biochem kit (BK105, Cytoskeleton) according to the manufacturer's instructions.

Statistical analysis:

Burden testing for RSVs seen in *ARHGAP5* or *ARHGAP35* individuals as compared to gnomAD was performed using Fisher's exact test.[16] Given the assessment of multiple regions of *ARHGAP35* for regional enrichment for missense variants, Bonferroni correction was applied to the p-value for RhoGAP missense variants. We used a student's *t*-test to detect statistical differences between zebrafish gene expression levels measured by qRT-PCR (biological triplicates). We used a one-way ANOVA with multiple comparison testing to compare GFP+ area and head size measurements across genotypes using GraphPad Prism 9 (biological triplicates). *In vitro* analysis of p190A-GAP assay WT compared to mutant using an unpaired student's *t*-test.

RESULTS

Identification of heterozygous *ARHGAP35* Protein-Truncating Variants in five IHH Pedigrees

In a single pedigree, Family 1, ES of three affected family members in two generations uncovered one heterozygous RSV of interest that was shared by all affected family members: *ARHGAP35* ([GenBank ID: NM_004491.4] c.3569_3570delAG, p.(Glu1190Glyfs*9); Figures 1–2; Table 1; Supplementary Tables 4-5; clinical phenotype of proband published as case 4[25]). Consistent with filtering criteria, this RSV was absent from gnomAD (v2.2.1; 4/11/2022), and *ARHGAP35* is highly constrained for both PTVs (LOEUF=0.057) and missense variants (Z-score>3.0).[10] There were no additional RSVs of interest segregating with IHH in Family 1. There were no segregating RSVs or CNVs in known IHH genes. Segregation analysis confirmed that the variant was present in all affected individuals but also present in one unaffected child, compatible with variable penetrance, a common phenomenon documented in IHH.[1]

Next, we examined ES data from 1,386 unrelated IHH probands in our cohort for additional RSVs in *ARHGAP35.* Four protein-truncating RSVs in *ARHGAP35* ([NM_004491.4] c.345delC, p.(Tyr116Ilefs*55); c.352A>T, p.(Lys118*); c.516del, p.(Asn173Thrfs*23); c.1800_1803del, p.(Val601Tyrfs*26)) were identified in Families 2–5 (Figures 1- 2; Table 1; Supplementary Figure 1; Supplementary Table 4). Similarly, the probands in Families 2–4 did not carry any rare PTVs in known IHH genes. Family 5's proband harbored a *TUBB3* [NM_006086.3] PTV (c.815G>A, p.Trp272*) of unknown significance (VUS): *TUBB3* PTVs have not been associated with human disease, and mouse modeling suggests no brain or reproductive defect from complete loss of *Tubb3.*[26,27] There were rare missense VUS in known IHH genes in Families 2 and 5 (Figure 1, Supplementary Tables 4-5). Family 2's proband harbors a heterozygous VUS in *FGFR1* c.2182G>A p.E728K in the tyrosine kinase domain which is predicted to be deleterious. Family 5's proband harbors a heterozygous missense VUS in *SEMA3A* ([NM_006080.2] c.2189G>A, p.Arg730Gln) that has been shown to have no effect on secretion or signaling activity of *Sema3A* in prior *in vitro* modeling and a novel heterozygous missense variant in *KLB* c.3086A>T, p.K1029I which according to SIFT is a low confidence, deleterious call.[28,29] To assess the pathogenic likelihood of protein-truncating RSVs in *ARHGAP35* contributing to IHH, we performed gene-based burden testing for PTVs. This analysis revealed a significant enrichment unadjusted p=3.1E-06 in IHH probands (n=1,387) compared to gnomAD controls (n=70,133).

Data Sharing Identified ARHGAP35 PTVs in IHH, Neonatal Hypogonadism, and DD

Three additional individuals with rare PTVs in *ARHGAP35* were identified using GeneMatcher[15] (Figures 1–2; Table 1; Supplementary Table 4). The proband from Family 13 had IHH and neonatal hypogonadism (unilateral cryptorchidism, microphallus) with an unreported PTV in *ARHGAP35* (c.2565C>A, p.(Tyr855*)). Family 14's proband, who is currently prepubertal, had evidence for neonatal hypogonadism (unilateral cryptorchidism, microphallus), left coronal craniosynostosis, and DD; he carries a previously unreported *de novo* PTV in *ARHGAP35* (c.3283_3286delinsT, p.(Val1095*)). Family 15's proband is

also prepubertal, has tall stature with advanced bone age, and has DD with a rare PTV in *ARHGAP35* (c.325C>T, p.(Arg109*)).

p190 RhoGAP zebrafish mutants display GnRH neuron defects.

Zebrafish (*D. rerio*) are a tractable model to study genes implicated in IHH.[3,4,30] To explore whether p190 RhoGAP influences the establishment of the GnRH neuronal network during early development, we generated and characterized zebrafish mutant models with a transgenic reporter marking the relevant neuronal population, *gnrh3*-expressing neurons [*tg(gnrh3:egfp)*].[22]

We identified the zebrafish orthologs of ARHGAP35 through reciprocal BLAST searches of the human protein with the translated zebrafish genome (Supplementary Figure 2a-b). The zebrafish genome harbors two paralogs of ARHGAP35, likely resulting from the major teleost genome duplication event[31] (*arhgap35a*: 80% similarity, 69% identity; *arhgap35b*: 78% similarity, 67% identity for human vs. zebrafish protein). Mining of publicly available transcriptomic datasets revealed that both transcripts are present from the zygote stage through larval day 5 (EMBL-EBI Expression Atlas). Notably, *arhgap35b* transcript has been reported at substantially lower levels in the zebrafish head than *arhgap35a* at 5 dpf (*arhgap35b* level 35% of *arhgap35a*)[32]; however, we could not exclude the possibility that both paralogs perform redundant and/or GnRH-relevant cellular roles and modeled both independently.

We used CRISPR/Cas9 genome editing to target both zebrafish genes in *tg(gnrh3:egfp)* embryos. We identified sgRNA targets in the coding regions, *in vitro* transcribed sgRNA, and co-injected with Cas9 protein in single-cell stage embryos. Founder (F0) mosaic mutants were grown to adulthood and outcrossed to adults harboring the *gnrh3:gfp* transgene to establish stable F1 heterozygous mutants. We isolated frameshifting variants in each transcript (*arhgap35a*:16 bp insertion resulting in p.His826Glnfs*34; *arhgap35b*: 7 bp insertion resulting in p.Asn1147Serfs*11; Supplementary Figure 2a-b). To validate whether each variant resulted in gene ablation, we performed F1 heterozygous in-crosses and monitored endogenous transcript levels using qRT-PCR starting from total RNA isolated from heads of homozygous mutants compared to WT siblings at 2 dpf. For both mutants, we observed significant reduction of endogenous transcript ($p<0.01$, Student's t-test; 28%, 40%of WT levels for *arhgap35a* and *arhgap35b* homozygous mutants, respectively; Supplementary Figure 2d).

After establishing significant gene disruption in each p190 RhoGAP zebrafish mutant, we quantified GnRH3-GFP+ cells with live automated imaging of fluorescent signal at 5 dpf in larvae resulting from heterozygous mutant adult in-crosses (Supplementary Table 7). Notably, we consistently observed expected Mendelian ratios for each of the mutant lines, arguing against the possibility of early lethality (Figure 3b, d; Supplementary Figure 3). Further, we observed no apparent developmental delay or other morphological defects in mutant animals (Supplementary Figure 3a, d). Measurement of GnRH3-GFP+ area on dorsal images revealed a significant reduction for *arhgap35a* homozygous mutants compared to WT ($p=0.0019$, one-way ANOVA; Figure 3a-b); with no detectable differences in head size area (Supplementary Figure 3a-c). However, we observed no differences between

arhgap35b homozygotes and WT counterparts (GnRH3-GFP+ area or head size). Notably, heterozygous *arhgap35a* animals do not display detectable GnRH phenotypes (Figure 3a, b), however this disparity between zebrafish and humans is well-recognized for several human genes implicated in Mendelian disease[33–35]. We speculate that genetic redundancy and/or genetic compensation in zebrafish likely results in genetic buffering that is different from humans[36].

Together, these data suggest that: (1) *arhgap35a*, the more highly conserved paralog that is more highly expressed in anterior structures, impacts the phenotype of a relevant GnRH neuronal population offering a mechanistic link between ARHGAP35 dysfunction and reproductive phenotype of our human cohort; and (2) *arhgap35b* does not appear to be necessary for GnRH3-GFP neuronal patterning in larval zebrafish.

Heterozygous *ARHGAP35* missense variants are only enriched in the RhoGAP domain in IHH

In addition to the PTVs, IHH subjects also harbor *ARHGAP35* missense variation, but significant enrichment was observed only for missense variants that affect the RhoGAP domain (adjusted p=4.9E-03; IHH cohort: n=6/2774 alleles; gnomAD: n=83/231350 alleles, RhoGAP domain missense in Figure 2; Table 1; Supplementary Tables 4-6). Expanding this analysis to include *ARHGAP35* p.P1433A with a maximum MAF in the Ashkenazi Jewish population of 0.39% does not change the observed enrichment (adjusted p=1E-04; IHH cohort: n=7/2774 alleles; gnomAD: n=126/231350 alleles). Notably, a single *de novo* missense variant previously published in a DD study also occurs in the RhoGAP domain (p.P1407S; Figure 2)[14], suggesting that RSVs affecting this domain may be pathogenic. Consistent with this finding, three of the seven *ARHGAP35* missense RSVs identified in our cohort are hitherto unreported, predicted deleterious by *in silico* programs (Polyphen-2; SIFT), and found in families with no other known IHH RSVs or CNVs (Figures 1–2, Supplementary Table 4-5) suggesting they likely to contribute to disease. Two of the seven families with missense RSVs in *ARHGAP35* harbored pathogenic RSVs or CNVs in *ANOS1* that explained their phenotypes (Family 8 and 10, Figure 1, Supplementary Table 4).

Missense Variants in *ARHGAP35* have variable impact on GAP Activity

The *in vitro* p190A-GAP assay evaluates the ability of the ARHGAP35 RhoGAP domain to enhance the rate of GTP hydrolysis by the small GTPase RhoA, a critical protein function[24]. To examine this function, WT p190A-GAP or the indicated mutant proteins were expressed as GST fusion proteins in *E. coli* for *in vitro* GAP assays. WT p190A-GAP and mutant proteins were purified and resolved by SDS-PAGE, showing efficient protein stability and solubilization (Supplementary Figure 4). As expected, RhoA showed little intrinsic GTPase activity alone while the addition of WT p190A-GAP significantly enhances the hydrolysis of GTP (Figure 4). On the contrary, the *ARHGAP35* p.(Arg1284Trp) variant, which occurs at the critical conserved “arginine finger,” demonstrated severely impaired phosphate release; thus confirming abolished GAP activity.[37] Control variants (p.(Arg1419Cys), p.(Asp1340Asn)) and case variants (p.(Met1412Thr), p.(Ala1414Thr), p.(Arg1350Gln), p.(Pro1433Ala)) in non-conserved residues[37] which were also seen in

gnomAD, all showed normal GAP activity. The other previously unreported *ARHGAP35* missense variants, p.(Pro1331Leu) and p.(His1369Asp), could not be tested because of insufficient purified protein amounts. However, since Pro1331 is a well conserved residue amongst the various RhoGAP proteins and His1369 is localized in the four-helix bundle of the RhoGAP domain[37], it is most likely that these variants cause protein misfolding and impaired GAP activity. This well-validated assay provides a read-out of ARHGAP35 GAP activity; however, because it utilizes just the RhoGAP domain *in vitro*, variants that result in conformational changes that alter the ability of the protein to bind targets or destabilize the protein could be inaccurately classified as benign.

ARHGAP35 RSVs are Inherited and Result in Variable Expressivity

Across all families in the IHH cohort, 50% of probands with IHH and *ARHGAP35* RSVs were anosmic. Fifty percent (5/10) of male probands reported in this study displayed severe neonatal hypogonadism as evidenced by microphallus and/or cryptorchidism. In addition, 2 of 5 individuals with IHH and PTVs in *ARHGAP35* underwent reversal of their hypogonadism in adulthood, resulting in normal gonadal function in the absence of medications. Regarding additional non-reproductive phenotypes, 3 of 14 individuals with IHH in 2 families reported learning disabilities (Table 1; Supplementary Table 4). For all individuals in the IHH cohort for which parental genotyping data is available, the ARHGAP35 RSV is inherited; although, the Family 14 proband from GeneMatcher with neonatal hypogonadism and DD had a *de novo* PTV.

Heterozygous *ARHGAP5* PTVs are present in two Kallmann syndrome Families

De novo analysis of ES data in 175 IHH trios revealed a previously unreported heterozygous RSV in *ARHGAP5* ([NM_001030055.1] c.2366dupC, p.(Phe790Ilefs*2)) in Family 16(Figure 5, Supplementary Table 4). *ARHGAP5* is the most closely related member to *ARHGAP35* (51% identity, 68% amino acid similarity in humans) and is highly constrained for PTV (LOEUF=0.263).[10] No additional protein-truncating “RSVs of interest” were found in Family 16. Examination of the larger KS cohort (IHH + anosmia, n = 702) revealed one additional previously unreported heterozygous PTV in *ARHGAP5* (c.1504delT, p.(Tyr502Metfs*3)) in Family 17. Identifying two KS probands with rare protein-truncating RSVs in *ARHGAP5* motivated us to test for gene-based burden which revealed a moderate enrichment for PTVs (unadjusted p=0.003) in KS probands (alleles=2/1402) compared to gnomAD controls (alleles=13/233254).[10]

Based on the modest enrichment for PTVs in *ARHGAP5* and given the *de novo* nature of one of the identified variants, we examined the relevance of *ARHGAP5* in our zebrafish model. We identified a single zebrafish ortholog of ARHGAP5 (*arhgap5:* 85% similarity, 73% identity for human vs. zebrafish amino acid sequence) through reciprocal BLAST searches of the human protein with the translated zebrafish genome that is present from zygote stage through larval day 5 (Supplementary Figure 2c; EMBL-EBI Expression Atlas). We used CRISPR/Cas9 genome editing to target *arhgap5* in *tg(gnrh3:egfp)* embryos, as described above for *ARHGAP35*. We isolated a frameshifting variant in *arhgap5*: 86bp insertion resulting in p.Val1038Metfs*6For mutants. We observed significant reduction of

endogenous transcript (p<0.01, Student's t-test; 47% of WT levels for *arhgap5* homozygous mutants; Supplementary Figure 2d).

After establishing significant gene disruption in *arhgap5* mutants, we quantified GnRH3-GFP+ cells with live automated imaging of fluorescent signal at 5 dpf in larvae resulting from heterozygous mutant adult in-crosses (Supplementary Table 7). Notably, we consistently observed expected Mendelian ratios for *arhgap5*, arguing against the possibility of early lethality (Figure 3f; Supplementary Figure 3). Further, we observed no apparent developmental delay or other morphological defects in mutant animals (Supplementary Figure 3g). Comparison of GnRH neuronal area in *arhgap5* homozygotes versus WT siblings did not reveal any significant differences with stringent testing (one-way ANOVA; Figure 3e-f; Supplementary Figure 3g-i); however, we noted a trend toward a reduced GFP+ area that was modestly significant using a pairwise comparison between these two genotypes only (Student's *t*-test; p<0.05). These data indicate that *arhgap5* might play a role in GnRH neuronal patterning but could not be captured using our current mutant model system and experimental parameters. Taken together with our human genetic data, these findings implicate *ARHGAP5* as a potential candidate contributor to IHH pathogenesis, but this assertion requires further human genetic validation.

ACMG Classification of *ARHGAP35* and *ARHGAP5* Variants

To determine how variants in *ARHGAP35* and *ARHGAP5* should be evaluated clinically, we incorporated the above results into ACMG criteria for classifying variants. [38] PTVs in *ARHGAP35* are likely pathogenic based on the human, *in vivo*, and population and computational data (Supplementary Table 5). In contrast, missense RSVs in the RhoGAP domain have variable interpretations. *ARHGAP35* p.(Arg1284Trp) is likely pathogenic, while p.(Ala1414Thr) and p.(Met1412Thr) are likely benign. The other four missense variants in *ARHGAP35* are VUS: p.(Pro1331Leu), p.(Arg1350Gln), p.(His1369Asp), and p.(Met1412Thr). For *ARHGAP5*, the *de novo* PTV is likely pathogenic (p.(Phe790Ilefs*2)), but the other PTV is a VUS (p.(Tyr502Metfs*3)).

STRING pathway analysis

To explore further the p190 RhoGAP interactors, we assembled protein-protein interaction data. STRING pathway analysis revealed high confidence interaction scores connecting ARHGAP35 to ARHGAP5 and to the semaphorin network through PLXNC1, PLXNB1 and SEMA4D. (Supplementary Figure 5). Seeding with known IHH genes (Supplementary Table 1) confirmed these findings and established connections for ARHGAP35 and ARHGAP5 to known IHH genes (*FGF17, KLB, FGFR1, FGF8, GNRH1, DUSP6*) (Supplementary Figure 6).

DISCUSSION

This study implicates p190 RhoGAPs, *ARHGAP35* and *ARHGAP5*, [7–11]in IHH. p190 RhoGAPs, mainly *ARHGAP35*, have been implicated previously in neurodegenerative diseases, DD, and human cancers.[14,39] Here, we report 14 individuals with IHH in 12 unrelated families who harbor different heterozygous protein-truncating or RhoGAP

missense variants in *ARHGAP35* in an autosomal dominant inheritance pattern who were identified from 1,387 families. We functionally validated the *ARHGAP35* PTVs and one missense change (p.Arg1284Trp). Through GeneMatcher, we report three additional PTVs in *ARHGAP35* in individuals with IHH, IHH-related phenotypes, and/or DD. We also report the discovery of 2 individuals with KS in 2 families with different PTVs in *ARHGAP5*. This report expands the biologic role of the p190 RhoGAPs into reproductive biology and implicates IHH as an *ARHGAP35*-related human disorder.

Among *ARHGAP35*-related human disorders described to date, germline RSVs similar to this study have only been reported once in humans with DD wherein *de novo ARHGAP35* variants were identified.[14] DD are clinically heterogeneous, common, and genetically characterized by an excess of *de novo* CNVs/RSVs.[14] The genetic characteristics of DD and IHH differ with regards to the inheritance mode and the distribution of *ARHGAP35* RSVs. In contrast to the *de novo* variation in the DD study, *ARHGAP35* RSVs in IHH identified in this study were predominantly inherited with incomplete/variable penetrance, a pattern consistent with other known genetic forms of IHH.[1] While a similar percentage of RSVs were missense in the two cohorts (58% IHH, 53% DD), ninety percent (9/10) of identified missense RSVs in DD were outside the RhoGAP domain; whereas only missense variants within the RhoGAP domain were enriched in IHH.[14] Precise determination of these seemingly overlapping ARHGAP35 allelic disorders (IHH and DD) is hindered by a lack of information about reproductive phenotypes in the DD cohort.[14] In this regard, it is notable that in 2/12 families with *ARHGAP35*-related IHH, neurodevelopmental phenotypes such as learning disabilities (dyslexia, dyspraxia, math learning disability) were present. Furthermore, through GeneMatcher, we identified a *de novo ARHGAP35* PTV in a child with signs of neonatal hypogonadism and autism with intellectual disability. Thus, our observations suggest a phenotypic overlap between the *ARHGAP35*-related disorders of DD and IHH and that DD and IHH may lie across a longitudinal phenotypic spectrum. Indeed *ARHGAP35* is expressed across fetal development in the brain: the hypothalamus, thalamus, amygdala, ventricular zone, and marginal zone.[40] Additional deep, longitudinal phenotyping and genetic analyses for all individuals with RSVs in *ARHGAP35* are needed to understand this pleiotropic phenomenon and to discern the extent to which IHH and DD represent *ARHGAP35*-related overlapping disorders across a phenotypic continuum.

Multiple animal models demonstrate neurodevelopmental phenotypes that support the observed pleiotropy in humans. In zebrafish, loss of *arhgap35a*, the predominant p190 RhoGAP in the zebrafish brain, resulted in reduced GnRH neuronal area. Supporting this observation, recent *in vitro* sequencing of human GnRH neurons identified *ARHGAP35* as part of a network of top 50 upregulated genes across GnRH neuronal development.[41] While GnRH neurons have not been examined in p190 RhoGAP mouse models, *ARHGAP35* is expressed in mouse GnRH neurons, and GnRH-containing fibers form paths caudally and rostrally around the anterior commissure (AC).[42,43] Mice with a homozygous truncated variant of *Arhgap35* die perinatally and demonstrate loss of AC and hippocampal commissures (HC), disorganized cerebral cortex, and agenesis of the corpus callosum (CC) due to neuronal misrouting as a result of impaired adhesion and adhesion-mediated signaling.[8,9] Defects in the AC, HC, and CC can result in DD phenotypes in humans, including the dyspraxia seen in this report in a patient with KS due to an

ARHGAP35 PTV.[7,44,45] In addition, a mouse model with the variant *ARHGAP35* p.L1396Q demonstrated hypoplastic and/or glomerulocystic kidneys,[24] which has not been observed in our IHH cohort or other animal models.[7] Further examination of reproductive, renal, and neuronal phenotypes across animal models, humans, and *ARHGAP35* variant type is needed to dissect the observed pleiotropy.

Our pathway analyses showed that *ARHGAP35* interacts with three known IHH genes, *SEMA3A*, *SEMA3F*, and *PLXNA1*[28,46–48], and two candidate IHH genes, *SEMA4D* and *PLXNB1.*[13] This raises the hypothesis that *ARHGAP35* may result in IHH through regulation of semaphorin signaling. The SEMA3A-F/neuropilin/PLXNA1 complex provides signal guidance for the vomeronasal axons along which GnRH neurons migrate.[13,48] Loss of this signaling results in GnRH neurons that cannot migrate past the cribriform plate into the brain in mice.[13,46,47] In addition, SEMA4D/PLXNB1 signaling stimulates GnRH-1 neuronal migration and regulates GnRH-1 expression in the hypothalamus.[13] Loss of this signaling results in reduced GnRH neuronal number in the hypothalamus along with decreased GnRH-1 expression resulting in impaired fertility in mice.[13] ARHGAP35 physically associates with both PLXNA1 and PLXNB1, and the RhoGAP activity of ARHGAP35 is needed for plexin signaling.[12] Knock-down of ARHGAP35 transcripts using siRNA: 1) reduces semaphorin-mediated repulsion of endothelial cells, a marker of semaphorin impact on migration, for Sema3A, Sema3F, and Sema4D; and 2) results in the loss of Sema4D-induced neurite outgrowth in PC12 neural cells.[12] Haploinsufficiency of *ARHGAP35* could result in decreased semaphorin/plexin signaling in SEMA3A, SEMA3F, and SEMA4D pathways resulting in impairment of GnRH neuronal migration and reduced neurite outgrowth. However, further studies will be needed to validate these putative downstream consequences relating to ARHGAP35 deficits.

Because of the pathogenicity of PTVs presented in this report, we would recommend screening of *ARHGAP35* in patients with IHH, regardless of the presence or absence of associated phenotypes. We recognize that only one missense variant in this study was deemed to be pathogenic, pointing to the need for additional investigation of these types of nucleotide changes. We also note gnomAD may have limitations as a control arm for gene-based burden testing. However, because IHH genes are characterized by variable penetrance, it is likely that disease causing variants are in gnomAD biasing any gene-based burden testing towards the null.

In conclusion, this study provides robust human genetic evidence and functional data implicating heterozygous PTVs in *ARHGAP35* and a single *ARHGAP35* missense variant as causal genetic drivers for IHH. ARHGAP35's role as a master regulator of multiple semaphorins may underlie the pathogenesis of the IHH phenotype. Phenotypic features of IHH patients with *ARHGAP35* variants and their prior association with DD strongly imply that *ARHGAP35* variants result in pleiotropic developmental phenotypes. Future research into the mechanisms of *ARHGAP35* pleiotropy and detailed phenotyping across multiple organ systems of individuals with *ARHGAP35* RSVs are needed to decipher the full extent of ARHGAP35-related human phenotypes.

Data Availability:

Deidentified individual level data has been shared in Figures, and Supplemental Tables and Figures. Sequencing data for variants in this manuscript are deposited into ClinVar (https://www.ncbi.nlm.nih.gov/clinvar/; SUB11458441).

Supplementary Material

Refer to Web version on PubMed Central for supplementary material.

Acknowledgments:

We are grateful to the IHH families for their support and willingness to participate in our research studies. We thank all providers who referred individuals for genetic research. We acknowledge Dr. Maxime Bouchard, McGill University, Montreal, Canada, for providing the pGEX-6P1 encoding GST-tagged GAP domain of p190A. We acknowledge Rebecca A. Rojas, Vanessa P.F. Lopes, and Nicole P. DiOrio for Data Curation. This research was made possible through access to the data and findings generated by the 100,000 Genomes Project (Proband 14). The 100,000 Genomes Project is managed by Genomics England Limited (a wholly-owned company of the Department of Health and Social Care). The 100,000 Genomes Project is funded by the National Institute for Health Research and NHS England. The Wellcome Trust, Cancer Research UK, and the Medical Research Council have also funded research infrastructure. The 100,000 Genomes Project uses data provided by patients and collected by the National Health Service as part of their care and support. EED is the Ann Marie and Francis Klocke, MD Research Scholar.

Funding:

This work was supported by US NIH grants P50HD028138 (S.B.S., W.F.C. & R.B.) and P50HD104224 (S.B.S., M.F.L., R.B.); NSERC RGPIN/04809–2017 (N.L-V.); and the NIHR Oxford Biomedical Research Centre (A.O.M.W.). M.F.L. is supported by 5K23HD097296. R.B. is supported by R01HD096324. G.J.F. was supported by the Crusader Internship Fund from The College of the Holy Cross. R.S.T. was supported by an MRC DTP studentship. The 100,000 Genomes Project and associated infrastructure are funded by the National Institute for Health Research and NHS England, the Wellcome Trust, Cancer Research UK, and the Medical Research Council.

REFERENCES

1. Balasubramanian R, Crowley WF Jr., Isolated GnRH deficiency: a disease model serving as a unique prism into the systems biology of the GnRH neuronal network. Mol Cell Endocrinol 2011;346(1–2):4–12. DOI: 10.1016/j.mce.2011.07.012. [PubMed: 21782888]
2. Laitinen EM, Vaaralahti K, Tommiska J, et al. Incidence, phenotypic features and molecular genetics of Kallmann syndrome in Finland. Orphanet J Rare Dis 2011;6:41. DOI: 10.1186/1750-1172-6-41. [PubMed: 21682876]
3. Shaw ND, Brand H, Kupchinsky ZA, et al. SMCHD1 mutations associated with a rare muscular dystrophy can also cause isolated arhinia and Bosma arhinia microphthalmia syndrome. Nat Genet 2017;49(2):238–248. DOI: 10.1038/ng.3743. [PubMed: 28067909]
4. Davis EE, Balasubramanian R, Kupchinsky ZA, et al. TCF12 haploinsufficiency causes autosomal dominant Kallmann syndrome and reveals network-level interactions between causal loci. Hum Mol Genet 2020;29(14):2435–2450. DOI: 10.1093/hmg/ddaa120. [PubMed: 32620954]
5. Rojas RA, Kutateladze AA, Plummer L, et al. Phenotypic continuum between Waardenburg syndrome and idiopathic hypogonadotropic hypogonadism in humans with SOX10 variants. Genet Med 2021;23(4):629–636. DOI: 10.1038/s41436-020-01051-3. [PubMed: 33442024]
6. Stamou MI, Cox KH, Crowley WF Jr. Discovering Genes Essential to the Hypothalamic Regulation of Human Reproduction Using a Human Disease Model: Adjusting to Life in the “-Omics” Era. Endocr Rev 2015;36(6):603–21. DOI: 10.1210/er.2015-1045. [PubMed: 26394276]
7. Brouns MR, Matheson SF, Hu KQ, et al. The adhesion signaling molecule p190 RhoGAP is required for morphogenetic processes in neural development. Development 2000;127(22):4891–903. (https://www.ncbi.nlm.nih.gov/pubmed/11044403). [PubMed: 11044403]

8. Brouns MR, Matheson SF, Settleman J. p190 RhoGAP is the principal Src substrate in brain and regulates axon outgrowth, guidance and fasciculation. Nat Cell Biol 2001;3(4):361–7. DOI: 10.1038/35070042. [PubMed: 11283609]
9. Matheson SF, Hu KQ, Brouns MR, Sordella R, VanderHeide JD, Settleman J. Distinct but overlapping functions for the closely related p190 RhoGAPs in neural development. Dev Neurosci 2006;28(6):538–50. DOI: 10.1159/000095116. [PubMed: 17028431]
10. Karczewski KJ, Francioli LC, Tiao G, et al. The mutational constraint spectrum quantified from variation in 141,456 humans. Nature 2020;581(7809):434–443. DOI: 10.1038/s41586-020-2308-7. [PubMed: 32461654]
11. Burbelo PD, Miyamoto S, Utani A, et al. p190-B, a new member of the Rho GAP family, and Rho are induced to cluster after integrin cross-linking. J Biol Chem 1995;270(52):30919–26. DOI: 10.1074/jbc.270.52.30919. [PubMed: 8537347]
12. Barberis D, Casazza A, Sordella R, et al. p190 Rho-GTPase activating protein associates with plexins and it is required for semaphorin signalling. J Cell Sci 2005;118(Pt 20):4689–700. DOI: 10.1242/jcs.02590. [PubMed: 16188938]
13. Messina A, Giacobini P. Semaphorin signaling in the development and function of the gonadotropin hormone-releasing hormone system. Front Endocrinol (Lausanne) 2013;4:133. DOI: 10.3389/fendo.2013.00133. [PubMed: 24065959]
14. Kaplanis J, Samocha KE, Wiel L, et al. Evidence for 28 genetic disorders discovered by combining healthcare and research data. Nature 2020;586(7831):757–762. DOI: 10.1038/s41586-020-2832-5. [PubMed: 33057194]
15. Sobreira N, Schiettecatte F, Valle D, Hamosh A. GeneMatcher: a matching tool for connecting investigators with an interest in the same gene. Hum Mutat 2015;36(10):928–30. DOI: 10.1002/humu.22844. [PubMed: 26220891]
16. Guo MH, Plummer L, Chan YM, Hirschhorn JN, Lippincott MF. Burden Testing of Rare Variants Identified through Exome Sequencing via Publicly Available Control Data. Am J Hum Genet 2018;103(4):522–534. DOI: 10.1016/j.ajhg.2018.08.016. [PubMed: 30269813]
17. Adzhubei I, Jordan DM, Sunyaev SR. Predicting functional effect of human missense mutations using PolyPhen-2. Curr Protoc Hum Genet 2013;Chapter 7:Unit7 20. DOI: 10.1002/0471142905.hg0720s76.
18. Choi Y, Sims GE, Murphy S, Miller JR, Chan AP. Predicting the functional effect of amino acid substitutions and indels. PLoS One 2012;7(10):e46688. DOI: 10.1371/journal.pone.0046688.
19. Schwarz JM, Cooper DN, Schuelke M, Seelow D. MutationTaster2: mutation prediction for the deep-sequencing age. Nat Methods 2014;11(4):361–2. DOI: 10.1038/nmeth.2890. [PubMed: 24681721]
20. Fu JM, Satterstrom FK, Peng M, et al. Rare coding variation illuminates the allelic architecture, risk genes, cellular expression patterns, and phenotypic context of autism. medRxiv 2021:2021.12.20.21267194. DOI: 10.1101/2021.12.20.21267194.
21. Szklarczyk D, Gable AL, Nastou KC, et al. The STRING database in 2021: customizable protein-protein networks, and functional characterization of user-uploaded gene/measurement sets. Nucleic Acids Res 2021;49(D1):D605–D612. DOI: 10.1093/nar/gkaa1074. [PubMed: 33237311]
22. Abraham E, Palevitch O, Gothilf Y, Zohar Y. The zebrafish as a model system for forebrain GnRH neuronal development. Gen Comp Endocrinol 2009;164(2–3):151–60. DOI: 10.1016/j.ygcen.2009.01.012. [PubMed: 19523393]
23. Labun K, Montague TG, Krause M, Torres Cleuren YN, Tjeldnes H, Valen E. CHOPCHOP v3: expanding the CRISPR web toolbox beyond genome editing. Nucleic Acids Res 2019;47(W1):W171–W174. DOI: 10.1093/nar/gkz365. [PubMed: 31106371]
24. Stewart K, Gaitan Y, Shafer ME, et al. A Point Mutation in p190A RhoGAP Affects Ciliogenesis and Leads to Glomerulocystic Kidney Defects. PLoS Genet 2016;12(2):e1005785. DOI: 10.1371/journal.pgen.1005785.
25. Quinton R, Cheow HK, Tymms DJ, Bouloux PM, Wu FC, Jacobs HS. Kallmann's syndrome: is it always for life? Clin Endocrinol (Oxf) 1999;50(4):481–5. DOI: 10.1046/j.1365-2265.1999.00708.x. [PubMed: 10468907]

26. Balasubramanian R, Chew S, MacKinnon SE, et al. Expanding the phenotypic spectrum and variability of endocrine abnormalities associated with TUBB3 E410K syndrome. J Clin Endocrinol Metab 2015;100(3):E473–7. DOI: 10.1210/jc.2014-4107. [PubMed: 25559402]
27. Latremoliere A, Cheng L, DeLisle M, et al. Neuronal-Specific TUBB3 Is Not Required for Normal Neuronal Function but Is Essential for Timely Axon Regeneration. Cell Rep 2018;24(7):1865–1879 e9. DOI: 10.1016/j.celrep.2018.07.029. [PubMed: 30110642]
28. Hanchate NK, Giacobini P, Lhuillier P, et al. SEMA3A, a gene involved in axonal pathfinding, is mutated in patients with Kallmann syndrome. PLoS Genet 2012;8(8):e1002896. DOI: 10.1371/journal.pgen.1002896.
29. Ng PC, Henikoff S. SIFT: Predicting amino acid changes that affect protein function. Nucleic Acids Res 2003;31(13):3812–4. DOI: 10.1093/nar/gkg509. [PubMed: 12824425]
30. Howard SR, Guasti L, Ruiz-Babot G, et al. IGSF10 mutations dysregulate gonadotropin-releasing hormone neuronal migration resulting in delayed puberty. EMBO Mol Med 2016;8(6):626–42. DOI: 10.15252/emmm.201606250. [PubMed: 27137492]
31. Postlethwait JH, Yan YL, Gates MA, et al. Vertebrate genome evolution and the zebrafish gene map. Nat Genet 1998;18(4):345–9. DOI: 10.1038/ng0498-345. [PubMed: 9537416]
32. Borck G, Hog F, Dentici ML, et al. BRF1 mutations alter RNA polymerase III-dependent transcription and cause neurodevelopmental anomalies. Genome Res 2015;25(2):155–66. DOI: 10.1101/gr.176925.114. [PubMed: 25561519]
33. Takamiya M, Stegmaier J, Kobitski AY, et al. Pax6 organizes the anterior eye segment by guiding two distinct neural crest waves. PLoS Genet 2020;16(6):e1008774. DOI: 10.1371/journal.pgen.1008774.
34. Liu H, Rigamonti D, Badr A, Zhang J. Ccm1 regulates microvascular morphogenesis during angiogenesis. J Vasc Res 2011;48(2):130–40. DOI: 10.1159/000316851. [PubMed: 20926893]
35. Teng CS, Ting MC, Farmer DT, Brockop M, Maxson RE, Crump JG. Altered bone growth dynamics prefigure craniosynostosis in a zebrafish model of Saethre-Chotzen syndrome. Elife 2018;7. DOI: 10.7554/eLife.37024.
36. Kontarakis Z, Stainier DYR. Genetics in Light of Transcriptional Adaptation. Trends Genet 2020;36(12):926–935. DOI: 10.1016/j.tig.2020.08.008. [PubMed: 32928563]
37. Jenna S, Lamarche-Vane N. The superfamily of Rho GTPase-activating proteins. In: Symons M, ed. RhoGTPases. New York: Kluwer Academic Press/Plenum Press; 2003:68–87.
38. Richards S, Aziz N, Bale S, et al. Standards and guidelines for the interpretation of sequence variants: a joint consensus recommendation of the American College of Medical Genetics and Genomics and the Association for Molecular Pathology. Genet Med 2015;17(5):405–24. DOI: 10.1038/gim.2015.30. [PubMed: 25741868]
39. Heraud C, Pinault M, Lagree V, Moreau V. p190RhoGAPs, the ARHGAP35- and ARHGAP5-Encoded Proteins, in Health and Disease. Cells 2019;8(4). DOI: 10.3390/cells8040351.
40. Dataset: Allen Institute for Brain Science. Allen Developing Human Brain Atlas: Microarray [dataset] Primary Publication: Miller, J. A., Ding, S.-L., et al. (2014). Transcriptional landscape of the prenatal human brain. Nature, 508(7495), 199–206. 10.1038/nature13185: Available from brainspan.org. RRID:SCR_008083; 2010. [PubMed: 24695229]
41. Lund C, Yellapragada V, Vuoristo S, et al. Characterization of the human GnRH neuron developmental transcriptome using a GNRH1-TdTomato reporter line in human pluripotent stem cells. Dis Model Mech 2020;13(3). DOI: 10.1242/dmm.040105.
42. Burger LL, Vanacker C, Phumsatitpong C, et al. Identification of Genes Enriched in GnRH Neurons by Translating Ribosome Affinity Purification and RNAseq in Mice. Endocrinology 2018;159(4):1922–1940. DOI: 10.1210/en.2018-00001. [PubMed: 29522155]
43. Merchenthaler I, Gorcs T, Setalo G, Petrusz P, Flerko B. Gonadotropin-releasing hormone (GnRH) neurons and pathways in the rat brain. Cell Tissue Res 1984;237(1):15–29. DOI: 10.1007/BF00229195. [PubMed: 6383617]
44. Siffredi V, Anderson V, Leventer RJ, Spencer-Smith MM. Neuropsychological profile of agenesis of the corpus callosum: a systematic review. Dev Neuropsychol 2013;38(1):36–57. DOI: 10.1080/87565641.2012.721421. [PubMed: 23311314]

45. Ridley B, Beltramone M, Wirsich J, et al. Alien Hand, Restless Brain: Salience Network and Interhemispheric Connectivity Disruption Parallel Emergence and Extinction of Diagonistic Dyspraxia. Front Hum Neurosci 2016;10:307. DOI: 10.3389/fnhum.2016.00307. [PubMed: 27378896]

46. Cariboni A, Davidson K, Rakic S, Maggi R, Parnavelas JG, Ruhrberg C. Defective gonadotropin-releasing hormone neuron migration in mice lacking SEMA3A signalling through NRP1 and NRP2: implications for the aetiology of hypogonadotropic hypogonadism. Hum Mol Genet 2011;20(2):336–44. DOI: 10.1093/hmg/ddq468. [PubMed: 21059704]

47. Marcos S, Monnier C, Rovira X, et al. Defective signaling through plexin-A1 compromises the development of the peripheral olfactory system and neuroendocrine reproductive axis in mice. Hum Mol Genet 2017;26(11):2006–2017. DOI: 10.1093/hmg/ddx080. [PubMed: 28334861]

48. Kotan LD, Ternier G, Cakir AD, et al. Loss-of-function variants in SEMA3F and PLXNA3 encoding semaphorin-3F and its receptor plexin-A3 respectively cause idiopathic hypogonadotropic hypogonadism. Genet Med 2021;23(6):1008–1016. DOI: 10.1038/s41436-020-01087-5. [PubMed: 33495532]

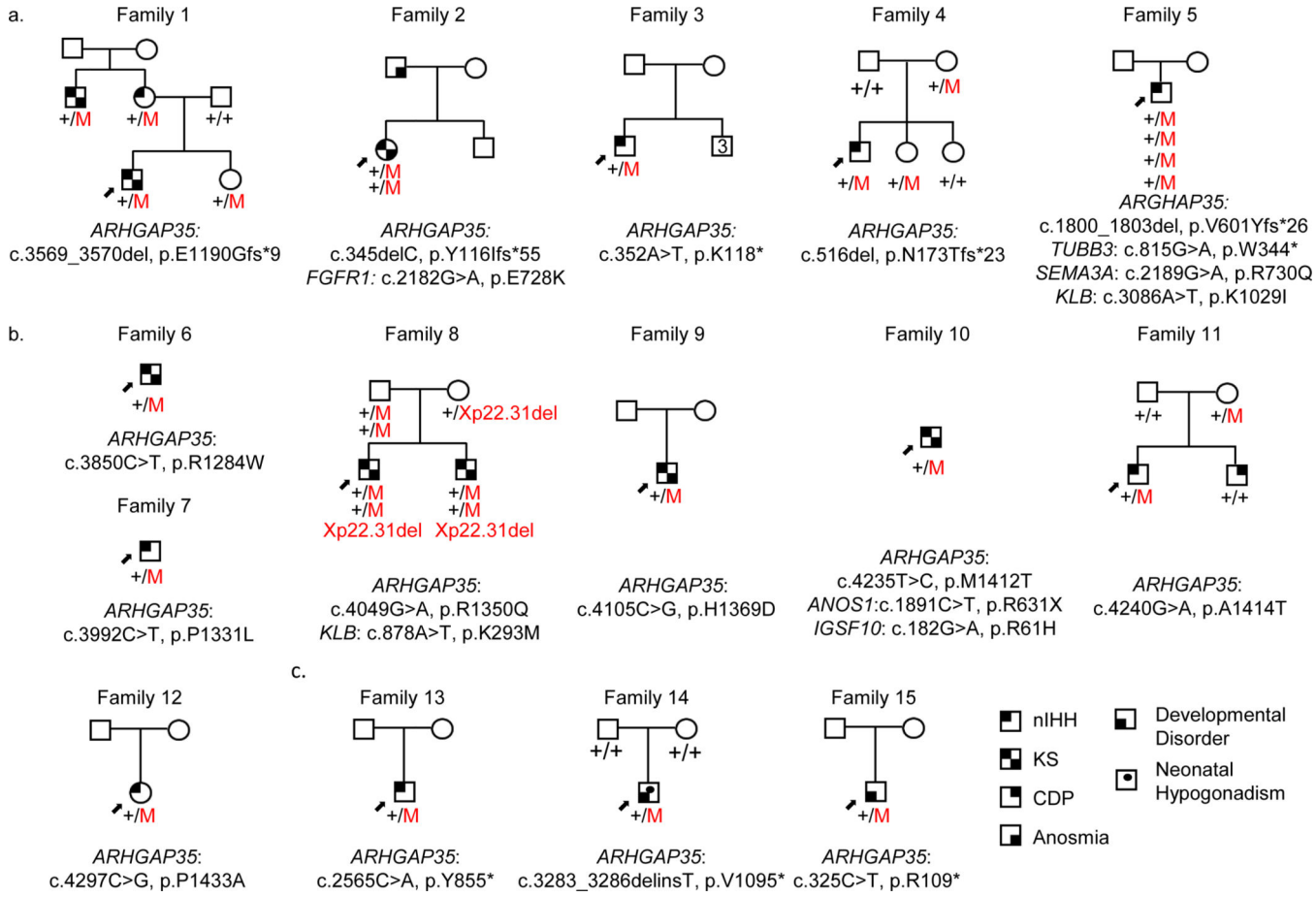

Figure 1. Pedigrees with rare *ARHGAP35* variants.

a. Loss of function variants; enrichment compared to controls, unadjusted p= 3.1E-06; b. RhoGAP domain missense variants; enrichment compared to controls, adjusted p=4.9E-3. c. GeneMatcher loss of function variants. Parents are shown when their phenotype is known. Abbreviations: “+”, wild-type allele; “M”, variant allele; nIHH, normosmic idiopathic hypogonadotropic hypogonadism; KS, Kallmann syndrome; CDP, constitutional delay of growth and puberty

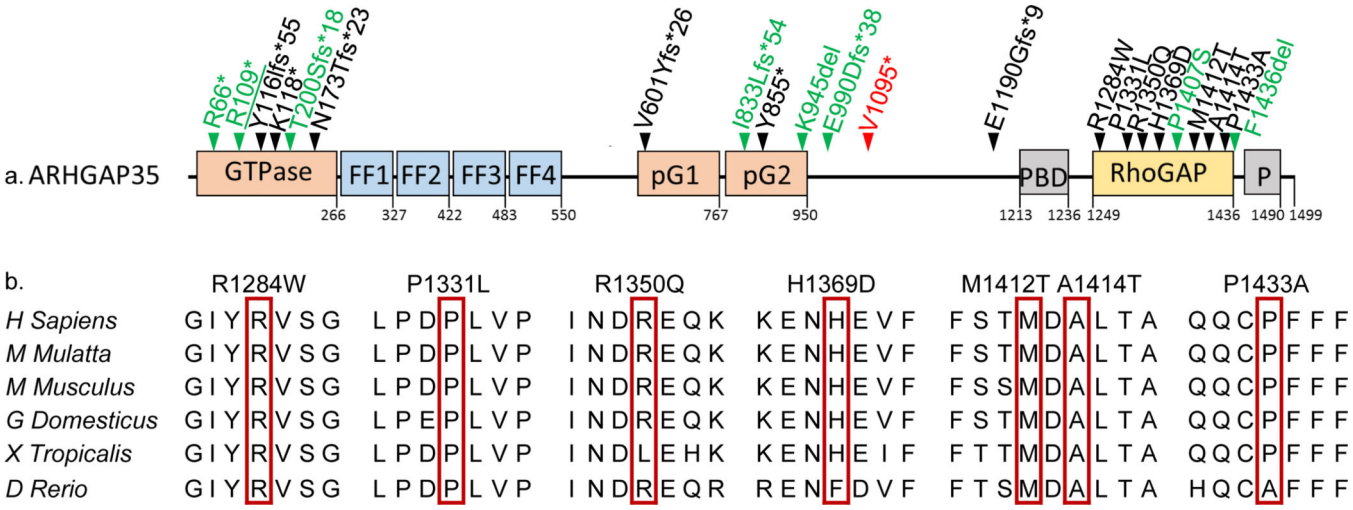

Figure 2. Rare variants identified in ARHGAP35.

a. Schematic of ARHGAP35 protein (GenBankID: NP_004482.4) and position of loss of function variants and RhoGAP domain missense variants (phenotypes: black – idiopathic hypogonadotropic hypogonadism (IHH), green – developmental disorder (DD) previously published, green underlined DD this report, red - neonatal hypogonadism and DD). FF, phenyalanine domains (blue); pG1, pseudo-GTPase domain 1 (salmon); pG2, pseudoGTPase domain 2 (salmon); PBD, phospholipid binding domain (gray); RhoGAP, Rho GTPase-activating proteins domain (yellow); P, proline rich domain (gray); amino acid position is labeled at the bottom. b. Conservation of missense variants identified in IHH in the RhoGAP domain across multiple vertebrate species.

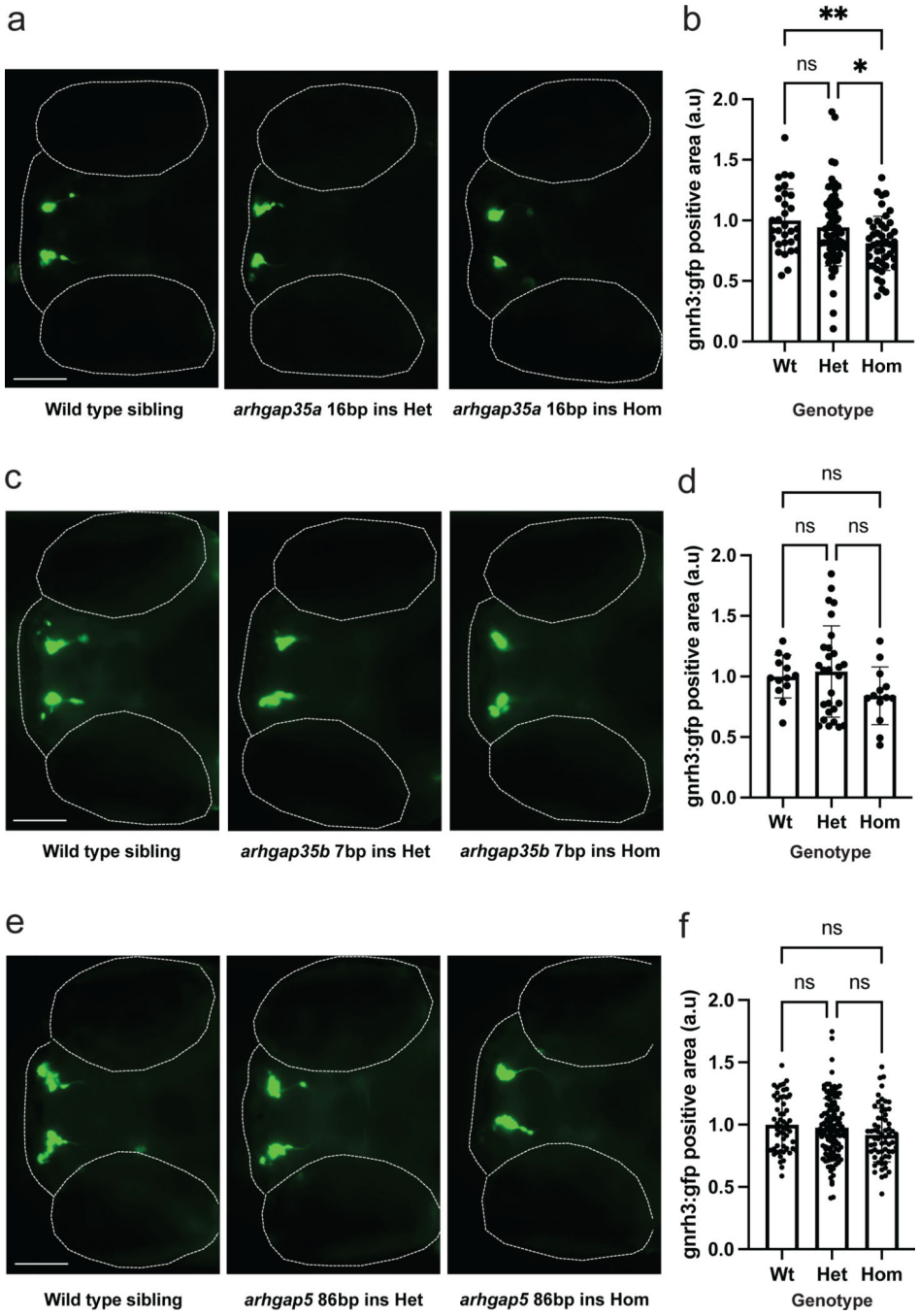

Figure 3. Characterization of GnRH3-GFP neuronal patterning in *arhgap35a*, *arhgap35b*, and *arhgap5* mutant zebrafish.

a, c, e. Representative dorsal images acquired from 5 dpf larvae to evaluate gnrh3:gfp signal. Anterior, left; posterior, right. Dotted lines indicate eyes and the most anterior region of the head. Scale bar, 100μm. b, d, f. Quantification of GnRH3-GFP+ signal in 5 dpf siblings compared across genotypes obtained from in-crosses of heterozygous mutant adults. Abbreviations: au, arbitrary units; WT, wild type; Het, heterozygous; Hom, homozygous; ns, not significant; significant differences detected with a one-way ANOVA; *p<0.05, **p<0.01; error bars indicate standard deviation.

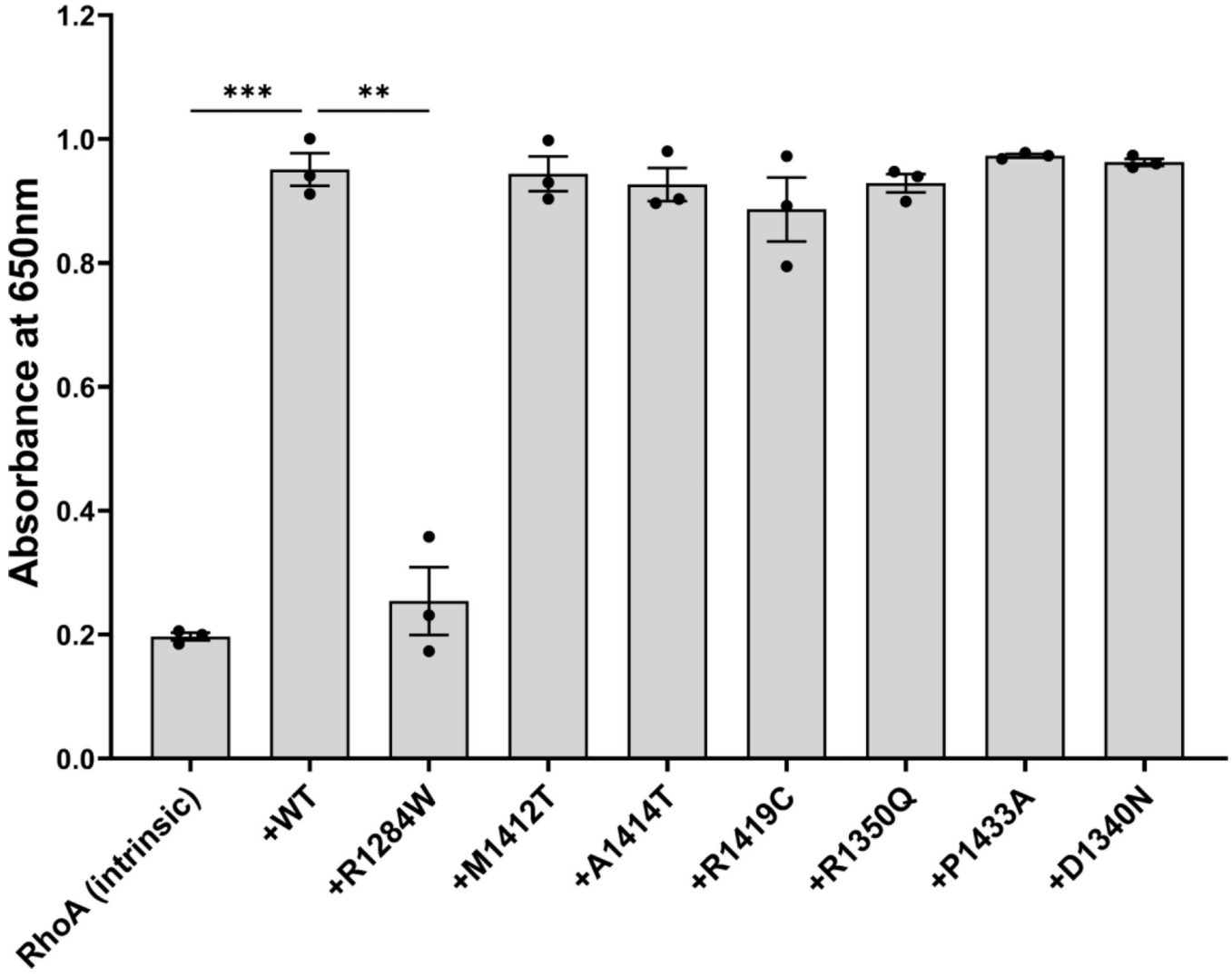

Figure 4: RhoGAP modeling of ARHGAP35 missense variants *in vitro*.

In vitro GAP activity assay towards RhoA in the absence (intrinsic) or presence of p190A-GAP wild type (WT) or mutant proteins. Arg1284Trp substitution is a loss-of-function variant in p190A GAP domain. Data are presented as mean ± S.E.M of three independent experiments (n=3). **, $p < 0.01$; ***, $p < 0.001$; unpaired student's t test.

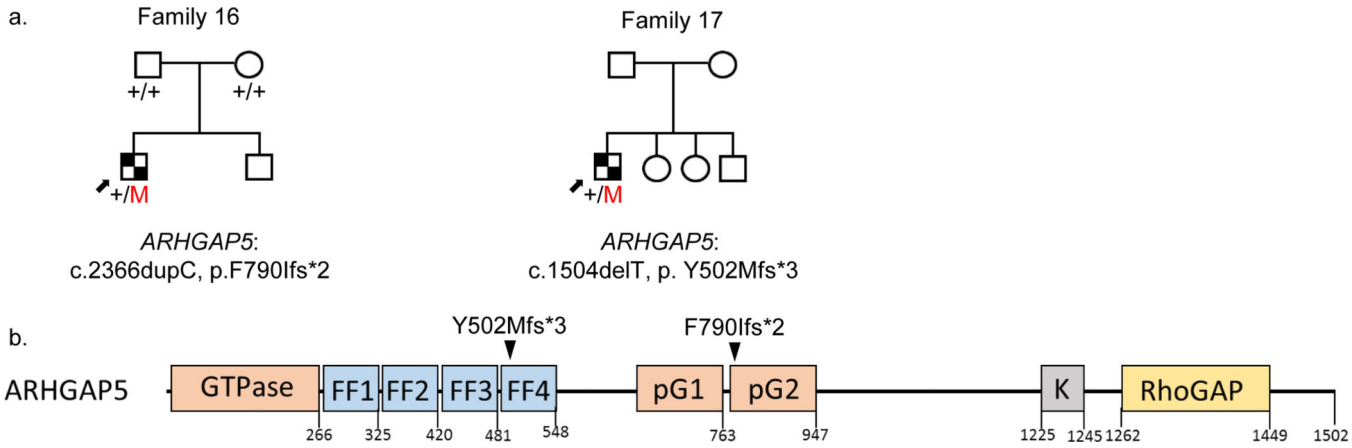

Figure 5: Kallmann Syndrome Pedigrees with rare *ARHGAP5* variants.

a. Pedigrees of probands with previously unreported loss of function variants. ”+”, wild-type allele; “M”, variant allele. b. Schematic of human ARHGAP5 protein (GenBank ID: NP_001025226.1) and position of variants identified in IHH cases. FF, phenyalanine domains (blue); pG1, pseudo-GTPase domain 1 (salmon); pG2, pseudoGTPase domain 2 (salmon); K, lysine rich domain (gray); RhoGAP, Rho GTPase-activating proteins domain (yellow); P, proline rich domain (gray); amino acid position is labeled at the bottom.

Table 1:

Phenotype of Individuals in this Study

					Reproductive phenotypes						Non-repr
Family	**Individual**	**Sex**	**Ethnicity**	**Age at Presentation**	**Diagnosis**	**Micropenis**	**Cryptorchidism**	**Reversal**	**Face/Head**	**Bone**	**Anosmia**
							ARHGAP35				
1	1	M	White	14[a]	KS	−	+[e]	−	−	−	+
	2	F	White	32	IHH	NA	NA	−	−	−	Mild microsmia
	3	M	White	17.7	KS	−	−	+	+	−	+
2	1	F	Asian	16[a]	KS	NA	NA	−	Deviated septum; Brachydactyly (type A3, R)	Osteopenia	+
3	1	M	White	21	IHH	+	+	+	−	Osteoporosis	ND
4	1	M	White	14	IHH	+	−	−	NR	NR	−
5[b]	1	M	White	NR	IHH	NR	NR	NR	NR	NR	−
6[b]	1	M	Brazilian	14[a]	IHH	−	−	−	−	−	ND
7[b]	1	M	White	NR	IHH	NR	+	NR	NR	NR	ND
8[b]	1	M	White	NR	KS	NR	NR	NR	NR	NR	+
	2	M	White	NR	KS	NR	NR	NR	NR	NR	+
9[b]	1	M	White	NR	KS	NR	+[e]	NR	NR	NR	+
10[b]	1	M	White	NR	KS	NR	−	NR	NR	NR	+
11	1	M	White	18.5	IHH	−	−	−	−	−	−
12[b]	1	F	White Hispanic	17[a]	IHH	NA	NA	−	High arched palate	Scoliosis	Hyposmia
13[c]	1	M	White	Adolescence[a]	IHH	+	+[e]	−	NR	Osteopenia, +2.5 SD	NR
14[c]	1	M	White	Neonatal period[d]	Neonatal hypogonadism, DD, CS	+	+[e]	NA	Left coronal CS, brachycephaly, epicanthic folds, nevus flammeus & diffuse haemangioma on scalp, uplifted earlobes, downward	ND	NA

					Reproductive phenotypes						Non-repr
Family	**Individual**	**Sex**	**Ethnicity**	**Age at Presentation**	**Diagnosis**	**Micropenis**	**Cryptorchidism**	**Reversal**	**Face/Head**	**Bone**	**Anosmia**
									slanting palpebral fissures		
15[c]	1	M	White	5[d]	Tall stature, DD	−	−	NA	Supernumerary incisor, Swallowing difficulties	Advanced by 2yrs at age 5, Weight +3 SD, Height +4SD	NA
							ARHGAP5				
16	1	M	White	14[a]	KS	+	−	−	−	Osteoporosis	+
17	1	M	White	15[a]	KS	−	−	−	Crowded teeth	−	+

Abbreviations: IHH = idiopathic hypogonadotropic hypogonadism, KS = Kallmann Syndrome (IHH + anosmia), NR = not reported, ND = not done, NA = not applicable, NL= normal, M= male, F=female, DD = developmental disorder, CS = craniosynostosis, ID = intellectual disability, CC = corpus callosum

[a] diagnosis confirmed after age 18;

[b] assessment by outside provider;

[c] identified through GeneMatcher;

[d] unable to assess for IHH as children are pre-pubertal;

[e] unilateral